Clays and Clay Minerals, Vol. 55, No. 4, 389–401, 2007.

WEATHERING SEQUENCES OF CLAY MINERALS IN SOILS ALONG A SERPENTINITIC TOPOSEQUENCE

Z. Y. Hseu[1,*], H. Tsai[2], H. C. Hsi[3] and Y. C. Chen[1]

[1] Department of Environmental Science and Engineering, National Pingtung University of Science and Technology, Nei-Pu, Pingtung 912-01, Taiwan
[2] Department of Geography, National Changhua University of Education, Changhua 50018, Taiwan
[3] Department of Safety, Health and Environmental Engineering, National Kaohsiung University of Science and Technology, Kaohsiung 811, Taiwan

Abstract—There has been limited research on clay mineral transformation in serpentinitic soils under humid tropical conditions. In this study, four soil pedons were selected along a toposequence from the summit (Entisol), shoulder (Vertisol), backslope (Alfisol) to footslope (Ultisol) positions to explore the contributions and the significance of landscape and weathering status of serpentinitic rock with regard to clay mineral transformations in eastern Taiwan. Experimental results indicated that the large amount of dithionite-citrate-bicarbonate-extractable Fe (Fe_d) and clay in the subsurface horizon were mainly caused by the strong leaching potential from intensive rainfall and weathering of the fine-grained parent rocks. The clay mineralogy reflected the clear weathering trend of the soils along the toposequence: (1) the soils on the summit and shoulder contained smectite and serpentine, which are predominant in the young soils derived from serpentinitic rocks; and (2) vermiculite gradually increased in the relatively old soils on backslope and footslope. The mineralogical transformations observed along the toposequence indicated that chlorite and serpentine, initially present in the Entisol on the summit, weather into smectite and interstratified chlorite-vermiculite in the intermediate soil on the shoulder under strong leaching and oxidizing conditions. Furthermore, vermiculite formed as the major weathering product of chlorite and smectite in the soil developed on the backslope. In addition to vermiculite, kaolinite and quartz formed in the soils on the footslope with the greatest concentration of Fe_d along the toposequence.

Key Words—Chlorite, Serpentine, Smectite, Soil Taxonomy, Taiwan, Toposequence, Weathering Sequence.

INTRODUCTION

Serpentinites are Mg-rich, sub-siliceous rocks formed primarily through the metamorphic alteration of dunite, peridotite or pyroxenite, and are composed chiefly of the serpentine minerals antigorite, chrysotile and lizardite (Istok and Harward, 1982). Serpentine minerals are relatively unstable in near-surface conditions and weather easily into other layer silicates, such as smectite and vermiculite (Rabenhorst *et al*., 1982; Dixon, 1989). Nevertheless, the serpentine minerals are stable in a few cases, particularly in the soils with high pH and $Mg^{2+}/Si(OH)_4$ activities (Dirven *et al*., 1976). The chemical weathering of these ultramafic rocks under tropical conditions has been studied extensively for their great nickel ore deposits (Golighty, 1981), but serpentine-derived soils attracted the interest of soil scientists for additional reasons. Serpentinitic soils display strong chemical fertility limitations owing both to a low Ca/Mg ratio and to high levels of non-anthropogenic Cr and Ni (Whittaker, 1954; Wilson and Berrow, 1978; Alexander *et al*., 1989; Bonifacio *et al*., 1997; Burt *et al*., 2001). Alexander (1988) also found that landscapes which developed from non-serpentinized ultramafic rocks were more stable than those from serpentinized rocks. In addition to plant-growth problems and landscape instabilities, environmental hazards associated with serpentinite include the presence of chrysotile asbestos in windblown materials and the potential release of Cr and Ni toxic metals to natural water systems during mineral weathering (Schreier *et al*., 1987; Cheshire and Güven, 2005).

Significant contributions to the understanding of weathering of serpentine minerals are found in pedological studies. For example, Wildman *et al*. (1968) concluded that serpentine minerals weathered to Fe-rich montmorillonite and that Mg was released during the temperate weathering processes. Rabenhorst *et al*. (1982) indicated that the weathering of serpentine minerals in temperate Hapudalfs tended towards the formation of smectite, which, with vermiculite, dominated the fine clay fractions. These were often interstratified with hydroxy-interlayered minerals. Serpentine minerals, although absent from the fine clay fractions, occurred with chlorite and vermiculite in the fine sandy fractions of the saprolite. Graham *et al*. (1990) also indicated that serpentine weathering prevails in an Argixeroll. The serpentine content of the sand fractions

* E-mail address of corresponding author:
zyhseu@mail.npust.edu.tw
DOI: 10.1346/CCMN.2007.0550407

decreased upward in the profile, whereas smectite, absent from the A horizons, increased with depth to a maximum in the C horizons. Bonifacio *et al*. (1997) demonstrated that serpentine could weather to low-charged vermiculite within well drained landscape positions and to smectite within poorly drained landscape positions. Lee *et al*. (2003) explored the genesis of weathering products in serpentinitic soils along a moisture regime gradient and indicated that chlorite transformed to vermiculite and interstratified chlorite-vermiculite with the progressive release of Mg from the brucitic sheet of the chlorite. Additionally, chlorite weathered into high-charged smectites whereas low-charged smectites were neoformed by precipitation of the elements released by serpentine weathering.

Ultramafic bodies cover <1% of the Earth's land surface, but are abundant in ophiolite belts along tectonic plate margins (Hamblin, 1992). Serpentine minerals are found extensively in the eastern part of Central Ridge and Costal Range in Taiwan, adjacent to the convergent boundary of Eurasia Plate and Philippine Sea Plate (Ho, 1988). Pedological studies of the mineral weathering sequence in the serpentinitic soils under humid tropical conditions, however, are relatively rare, in particular studies regarding the influence of landscape and weathering of the serpentinitic soils on clay mineral transformation. Therefore, the aims of this work are to: (1) identify the primary and secondary minerals throughout the serpentinitic soil profiles; (2) examine the relationships between the properties of the serpentinitic soils and their mineralogy; and (3) explore the transformation processes of clay minerals in the soils along a serpentinitic toposequence in Taiwan.

MATERIALS AND METHODS

Site description

Tong-An Mountain (N 23º03′04″, E 121º11′58″) is located in eastern Taiwan where the geology is characterized by arc-continent collision (Ho, 1988). The area studied consists of serpentinites and mudstones which belong to the Lichi formation and crop out in the southeastern part (Figure 1). The serpentinitic rocks are the exotic blocks of ophiolite from the Phillipine Sea Plate. The climate of the study area is characterized by high temperature and humidity, massive rainfall and tropical cyclones in summer.

Four soil pedons with slopes ranging from 5 to 15% and with good drainage were selected to reflect the potential development of soils on different landscape positions along a serpentinitic toposequence (Figure 1). Additionally, mudstone saprolite was also sampled at the 'A' point from the marginal toeslope on the above toposequence but within the mudstone matrix of the Lichi Formation. All pedons are approximately west-facing with Pedon TA-1 located on the summit, Pedon TA-2 on the shoulder, Pedon TA-3 on the backslope, and Pedon TA-4 on the footslope. Surprisingly, the toposequence is only ~150 m long, but contains four Soil Orders in Soil Taxonomy (Soil Survey Staff, 2006), ranging from Entisols to Ultisols. From the pedological point of view, the order of soil development was Pedon

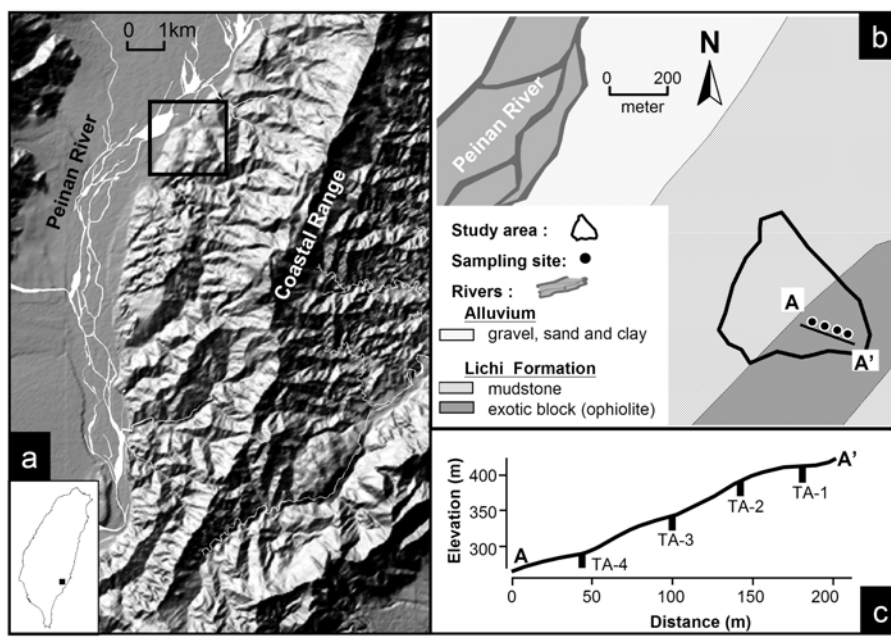

Figure 1. The study area: (a) location of Tong-An Mountain; (b) stratigraphic conditions and hillslope; (c) soil pedons along the toposequence.

TA-1 (Entisol) → Pedon TA-2 (Vertisol) → Pedon TA-3 (Alfisol) → Pedon TA-4 (Ultisol) (Hseu, 2006).

Physical and chemical analysis

Soil samples were collected from each horizon for physical and chemical analyses. The pH was measured using a mixture of soil and deionized water (1:1, w/v) with a glass electrode (McLean, 1982). The total organic carbon (OC) content was determined *via* the Walkley-Black wet oxidation method (Nelson and Sommers, 1982). Exchangeable cations and cation exchange capacity (CEC) were determined by the ammonium acetate method (pH 7.0) (Rhoades, 1982), and free Fe (Fe_d) was extracted by the dithionite-citrate-bicarbonate (DCB) method (Mehra and Jackson, 1960). The elemental compositions of the soils were determined by X-ray fluorescence (XRF) spectrometry. Finally, soil particle-size distribution was determined by the pipette method (Gee and Bauder, 1986).

Thin-section preparation and description

Kubiena boxes were used to collect rock and undisturbed soil blocks in the field for micromorphological studies. After air drying, vertically oriented thin-sections 30 μm thick were prepared by Spectrum Petrographics, Inc., Washington, USA; the sections were examined under polarized light in an optical microscope and described according to the terminology of Bullock *et al*. (1985).

X-ray diffraction of soil fraction and rock

Air-dried soil samples were pretreated with 30% H_2O_2 to remove any organic matter, and then treated with DCB to remove the Fe oxide coatings. The sand fraction (0.05−2 mm) was obtained using the wet sieve procedure; the silt (2−50 μm) and clay (<2 μm) fractions was extracted using continuous flow centrifugation. X-ray diffraction (XRD) analysis was performed on the oriented K- and Mg-saturated clay samples. The expansion properties of the Mg-saturated samples were determined by glycerol solvation at 65ºC for 24 h. The K-saturated samples were further subjected to successive heat treatments at 110ºC, 350ºC, and 550ºC for 2 h. The oriented clays were examined using an X-ray diffractometer (Rigaku D/max-2200/PC, Japan) and Ni-filtered CuKα radiation generated at 30 kV and 10 mA. The XRD patterns were recorded over the range 2−60º2θ with a scanning speed of 1.0º2θ/min. According to the reciprocal mineral intensity factors summarized by Kahle *et al*. (2002), the semi-quantitative determination of the clay minerals was based on the difference of reflection patterns from the K-saturated, Mg-saturated, glycolated, heated and air-dried samples (Johns *et al*., 1954).

The unweathered rock, sand and silt fractions of the soil were also examined as random powders by XRD with the same instrumental conditions as above.

Thermogravimetric analysis

The clay fraction was studied by thermogravimetric analysis after organic matter and Fe oxides were removed. The initial sample mass of ~10 mg was placed in a quasi-hemispherical platinum crucible (4 mm deep and 9 mm in cross-sectional diameter at its mouth). The thermobalance (Thermo Cahn model TG-2121, USA) was operated under a carrier gas flow of ultrahigh pure N_2 at 50 cm^3/min. The operating temperatures ranged from 20 to 1000ºC at a heating rate of 5ºC/min. The differential thermogravimetric (DTG) results could then be obtained based on the TG curves.

RESULTS AND DISCUSSION

Parent materials and primary minerals

The parent material of Pedons TA-1 and TA-2 is the residuum of exotic blocks of serpentinite underlain by the mudstone matrix of the Lichi Formation during the Pliocene and Pleistocene. However, the colluvium (weathered serpentine) over the residuum from serpentinite was transported and deposited as the parent material of Pedons TA-3 and TA-4. Therefore, the soils of Pedons TA-1 and TA-2 were weakly developed, but those of Pedons TA-3 and TA-4 were relatively more developed, by field observation.

The chrysotile, antigorite and lizardite of the serpentine mineral group have similar [$Mg_3Si_2O_5(OH)_4$] composition (Dixon, 1989; Caillaud *et al*., 2006). Three polymorphs of serpentine were clearly identified under the microscope by different textures. Veins of cross-fiber chrysotile are alternated with antigorite/lizardite in the serpentinitic rock (Figure 2a). The vein chrysotile is orange or brownish yellow with high birefringence (Figure 2b). The groundmass serpentine was further identified as antigorite from cross-foliated textures, and as lizardite from hourglass textures (Figure 2c). Caillaud *et al*. (2004, 2006) indicated that the hourglass textures were derived from olivine, and the cross-foliated (thin blades) textures were from pyroxene and amphibole in the serpentinite. Opaque inclusions of magnetite and chromite stain the parent rock brown or yellow (Figure 2d). Small amounts of weakly anisotropic light-yellow clay pseudomorphs, and irregularly distributed strong-yellow clayey material in voids or on the grain surfaces were interpreted as hypogene neoformed clay minerals (Figure 2d).

A rock sample powder XRD pattern shows reflections at 1.4, 0.71, 0.47, 0.35 and 0.28 nm, which are indicative of chlorite (Figure 3). Additional reflections at 0.73, 0.45, 0.36, 0.27 and 0.24 nm are characteristic of serpentine. The associated minerals including talc, magnetite and chromite were identified by the moderate peaks at 0.94, 0.49 and 0.31 nm for talc and the relatively clear peaks at 0.29 and 0.25 nm for magnetite and chromite, respectively, as previously observed by Nesse (2000) and Becquer *et al*. (2006). Residual

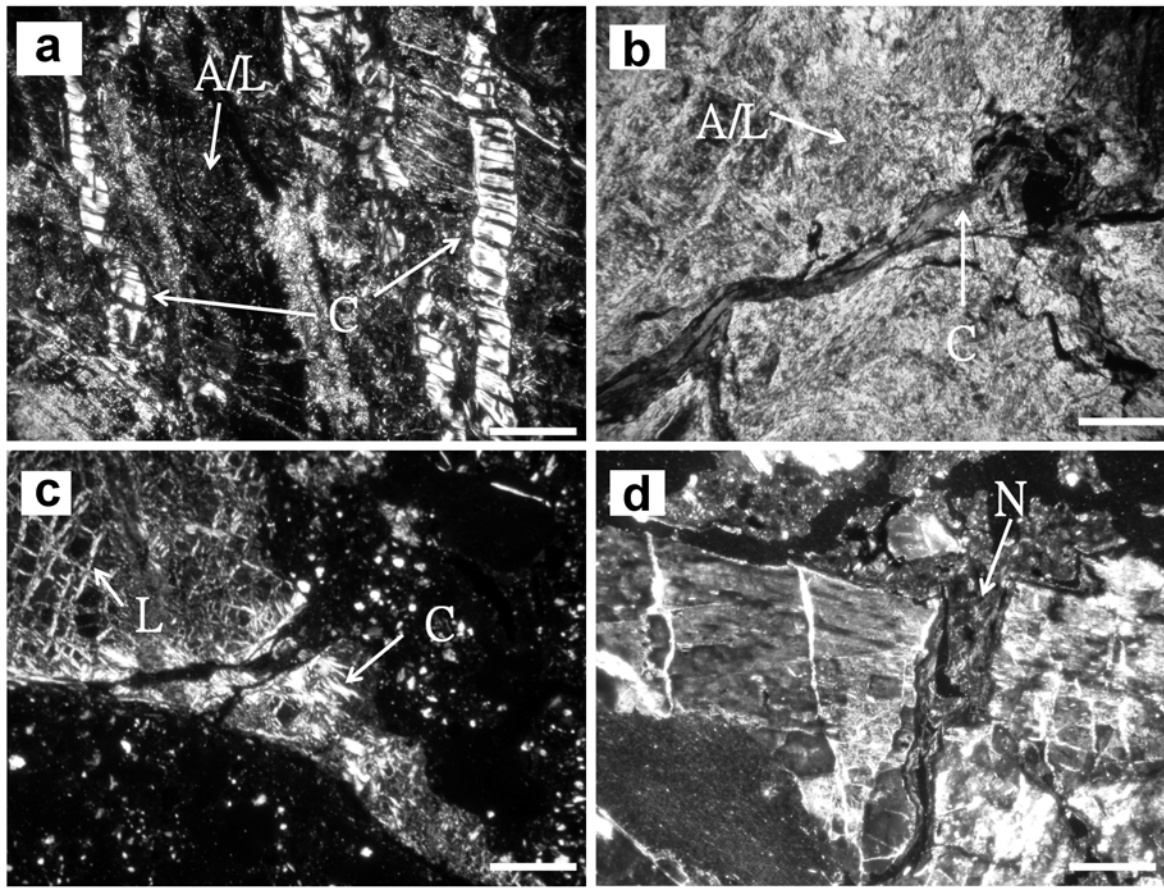

Figure 2. Micrographs of the thin-section of the serpentinitic rocks: (a) veins of chrysotile (C) alternated with antigorite/lizardite (AL) under cross-polarized light; length of scale bar is 0.125 mm; (b) chrysotile (C) with high birefringence throughout the groundmass of antigorite/lizardite (AL) under cross-polarized light; length of scale bar is 0.25 mm; (c) hourglass-textured lizardite (L) and fibrous chrysotile (C) under cross-polarized light; length of scale bar is 0.08 mm; (d) weakly anisotropic clay pseudomorphs in voids or on the grain surfaces as hypogene, neoformed clay minerals (N) including magnetite and chlorite under cross-polarized light; length of scale bar is 0.25 mm.

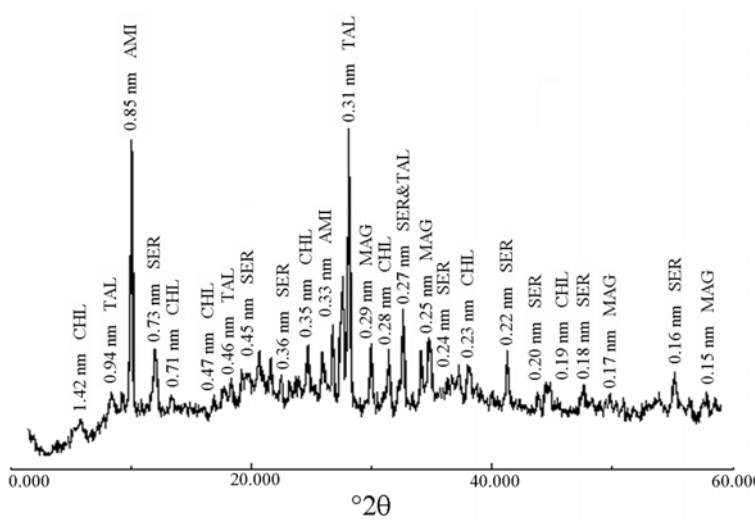

Figure 3. XRD powder pattern of the unweathered rock sample. CHL: chlorite; SER: serpentine; AMI: amphibole; MAG: magnetite; TAL: talc. CuKα radiation.

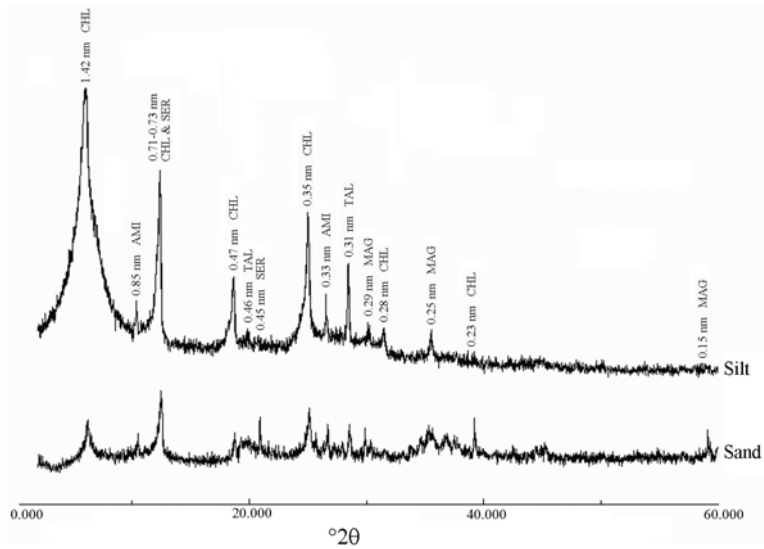

Figure 4. XRD patterns of silt and sand fractions of the BC1 horizon of Pedon TA-2. CHL: chlorite; SER: serpentine; AMI: amphibole; MAG: magnetite; TAL: talc. CuKα radiation.

amphibole was also identified in the parent rock by reflections at 0.85, 0.33 and 0.27 nm. The above-mentioned mineral species observed in the unweathered rock sample are also found in the sand and silt fractions of the initial and intermediate developed soils whereas the primary minerals mainly include chlorite, serpentine and amphibole, such as in Pedon TA-2 (Figure 4). However, the amounts of serpentine and amphibole are reduced in relatively highly developed soils, such as in Pedon TA-4. Nevertheless, the abundance of chlorite increased from unweathered rock to silt fraction of the soils.

Selected physical and chemical properties of the soil pedons

During the weathering, serpentine minerals are unstable in soil environments (Rabenhorst *et al*., 1982; Dixon, 1989), and are characterized by fine textures in microscopy. This is also perhaps due to the fine-grained nature of the parent materials. All the soils are well drained and have thick (>10 cm) A horizons with large clay content. The Munsell colors of the Aa-C1-C2 horizon sequence in Pedon TA-1 are very dark gray (10YR 3/1), dark brown (7.5YR 3/2) and strong brown (7.5YR 5/6). The colors of the other pedons resemble those of Pedon TA-1, but some of their subsurface horizons display 5YR or redder colors with more extensive degrees of pedogenesis. In Pedon TA-2, wide and deep cracks are found in the soil surface, and significant slickensides are found on the pedsurface of the B horizon. These field morphological characteristics meet the criteria in order to be classified as a Vertisol (Soil Survey Staff, 2006). Additionally, significant accumulation of illuvial clay is identified by optical observation of oriented argillans in Pedons TA-3 and TA-4 which have relatively shallow slopes. The soils in general have undergone intensive weathering and extensive leaching, resulting in metal and clay translocation. Meanwhile, the soil textures reveal large clay contents, especially in the subsurface horizons of all pedons (Table 1). The concentrations of DCB-extractable Fe (Fe_d) are normally greater in the B horizons of the soil profile (Table 1). The accumulation of illuvial clay and Fe_d in the subsurface horizon was mainly caused by the strong leaching potential of the very large amount of rainfall in the study area, especially in summer. The Fe_d content in mudstone saprolite on the toeslope is much less than those in all four soil pedons. The pH values were <7.0 in all the soils and generally increased with soil depth in Pedons TA-3 and TA-4 attributed to base cation accumulation in the lower parts of pedon. The soils derived from ultramafic rocks usually show high CEC values, as observed in this study, ranging from 26 to 74 cmol/kg. This indicated that very active colloids such as smectite and vermiculite existed in the soils. The OC content was always <4.0%. The percentage base saturation (PBS) of the diagnostic horizon in Pedon TA-3 generally exceeds 35%, while in Pedon TA-4 it is always significantly <35% (Table 1).

Therefore, Pedon TA-3 is classified as an Alfisol and TA-4 is classified as an Ultisol, according to the requirements of PBS and the argillic horizon defined in Soil Taxonomy (Soil Survey Staff, 2006). Although Pedon TA-4 is located on the well drained footslope, base cations are further released to the toeslope, the final sink of the cations. This result is in agreement with the report by Garnier *et al*. (2006) who indicated that the soils on the footslope were Ferralsols which equilibrated with Ultisols. Additionally, Bonifacio *et al*. (1997) had also identified four soil orders of the Soil Taxonomy along a short serpentinitic catena <100 m long, including Entisols, Inceptisols, Mollisols and Alfisols. Lee *et al*.

Table 1. Selected physical and chemical properties of the studied soils.

Horizon	Depth (cm)	Texture Sand (%)	Silt (%)	Clay (%)	pH	OC[1] (%)	CEC[2] (cmol(+)/kg)	PBS[3] (%)	Fe_d[4] (g/kg)
TA-1 (Summit: Typic Udorthent)									
Aa	0–18	18	47	35	6.6	0.9	39.9	89	8.92
C1	18–51	35	31	34	6.4	0.4	69.3	90	16.4
C2	51–90	40	27	33	6.3	0.2	74.2	90	20.6
TA–2 (Shoulder: Typic Hapludert)									
Aa	0–10	32	32	36	6.5	2.9	32.0	35	14.0
AB	10–30	41	26	33	6.4	2.2	27.4	60	15.3
Bss1	30–65	27	22	52	6.0	1.5	36.3	66	14.6
Bss2	65–94	28	15	58	6.0	1.2	34.6	55	19.7
Bss3	94–120	25	20	56	6.0	1.0	40.3	59	28.8
Bss4	120–145	34	24	53	6.2	1.0	35.5	55	12.2
Bss5	145–165	24	26	50	6.0	0.8	37.8	57	16.3
BC1	165–200	42	21	37	6.1	0.7	51.1	61	13.4
BC2	>200	34	25	41	6.0	0.8	36.3	62	14.2
TA-3 (Backslope: Typic Paleudalf)									
Ae	0–19	16	49	35	5.2	2.4	34.7	37	32.1
Bt1	19–48	8	40	53	5.1	1.2	41.9	44	34.5
Bt2	48–72	13	17	70	5.1	1.5	41.5	46	43.8
Bt3	72–101	12	23	65	5.3	0.8	50.9	45	45.5
Bt4	101–140	19	31	50	5.9	0.4	50.5	56	33.8
Bt5	140–170	22	32	47	6.1	0.6	49.7	57	22.7
Bt6	170–200	37	31	32	6.2	0.3	53.8	55	16.3
BC1	200–240	47	28	25	6.6	0.7	42.7	52	6.73
BC2	240–280	41	33	26	6.7	0.6	52.5	53	6.22
C	280–300	48	31	21	6.7	0.6	42.9	50	5.90
TA-4 (Footslope: Typic Paleudult)									
Ae	0–14	19	53	28	5.7	3.6	26.2	12	31.8
Bt1	14–60	19	31	50	4.8	1.4	27.7	6.0	69.4
Bt2	60–92	13	36	52	4.8	1.0	34.3	10	66.0
Bt3	92–125	16	41	44	5.1	0.9	31.9	9.0	49.0
Bt4	125–160	21	30	49	5.3	0.7	33.7	10	48.1
BC1	160–200	32	35	34	5.4	0.6	30.7	24	29.9
BC2	200–240	26	41	33	5.6	0.9	29.7	15	10.7
BC3	240–280	42	33	25	5.7	0.8	34.8	12	9.24
C	280–300	42	32	26	6.0	0.9	31.3	15	5.11
Mudstone saprolite (toeslope)									
		2	49	49	6.7	1.05	25.6	77	2.00

[1] Organic carbon
[2] Cation exchange capacity
[3] Percentage of base saturation
[4] Free Fe

(2004) indicated the pedogenesis of Mollisols and Alfisols in a serpentinitic terrain over the short distance of only 80 m.

The bulk chemical compositions of the different horizons in the four soil pedons show small Si contents in relation to the Si-poor mineralogy of the parent rock (Table 2). The total Mg contents are much greater than the Ca contents in the four pedons. The soils of Pedons TA-3 and TA-4 show larger Ca/Mg ratios than in the Pedons TA-1 and TA-2, in agreement with Alexander *et al*. (1989) who demonstrated that evolved serpentinitic soils showed higher Ca/Mg ratios because of strong Mg leaching. The Ni and Cr contents in these soils are greater than in soils formed from other parent materials, with considerable variation between the pedons in different landscapes (Table 2), which probably reflects the degrees of chemical weathering in the serpentinitic rocks (Lee *et al*., 2004; Massoura *et al*., 2006). The total Ni content follows the trend Pedon TA-2 > Pedon TA-1 > Pedon TA-4 $\geqslant$ Pedon TA-3. Colluvial materials over the residuum from serpentinitic rocks, mixed to a small extent with gray muddy sediments, were transported and deposited as the parent material of Pedons TA-3 and TA-4. Therefore, the total Ni contents in the soils of

Table 2. Total metal contents (wt.%) of the four soil pedons.

Horizon	Depth (cm)	Si	Al	Fe	K	Na	Ca	Mg	Mn	Cr	Ni
TA-1 (Summit: Typic Udorthent)											
Aa	0–18	30.3	0.49	8.37	0.32	0.13	0.02	1.70	0.15	0.16	0.27
C1	18–51	34.3	0.38	9.72	0.34	0.14	0.03	1.77	0.18	0.31	0.34
C2	51–90	37.1	0.55	7.37	0.48	0.14	0.02	2.59	0.15	0.26	0.27
TA-2 (Shoulder: Typic Hapludert)											
Aa	0–10	28.3	0.46	9.90	0.22	0.11	0.04	1.35	0.15	0.21	0.22
AB	10–30	27.5	0.64	10.3	0.22	0.11	0.08	1.75	0.19	0.18	0.23
Bss1	30–65	29.0	0.50	9.81	0.25	0.11	0.05	2.00	0.19	0.27	0.52
Bss2	65–94	29.5	0.58	10.7	0.25	0.12	0.05	1.41	0.21	0.18	0.54
Bss3	94–120	28.0	0.81	14.1	0.27	0.12	0.05	1.68	0.22	0.22	0.58
Bss4	120–145	28.8	0.38	12.1	0.24	0.12	0.04	2.04	0.21	0.27	0.58
Bss5	145–165	30.0	0.62	10.1	0.35	0.12	0.05	2.18	0.20	0.17	0.47
BC1	165–200	33.0	0.58	11.0	0.34	0.12	0.05	2.32	0.14	0.19	0.43
BC2	>200	29.6	0.81	12.2	0.36	0.12	0.04	2.31	0.15	0.17	0.42
TA-3 (Backslope: Typic Paleudalf)											
Ae	0–19	28.9	0.51	8.53	0.25	0.10	0.04	0.81	0.13	0.14	0.13
Bt1	19–48	27.9	0.63	8.97	0.25	0.13	0.05	1.13	0.14	0.10	0.13
Bt2	48–72	28.5	0.11	9.80	0.22	0.18	0.03	0.84	0.14	0.14	0.14
Bt3	72–101	28.2	0.17	11.0	0.24	0.12	0.03	1.02	0.14	0.14	0.14
Bt4	101–140	30.4	0.12	9.21	0.22	0.18	0.03	0.62	0.13	0.13	0.13
Bt5	140–170	28.3	0.12	8.48	0.34	0.17	0.01	1.07	0.13	0.13	0.12
Bt6	170–200	27.5	0.12	10.3	0.34	0.13	0.03	0.82	0.11	0.12	0.12
BC1	200–240	31.6	0.82	10.7	0.36	0.11	0.02	0.75	0.10	0.09	0.22
BC2	240–280	31.2	0.78	10.5	0.33	0.14	0.03	1.42	0.11	0.12	0.32
C	280–300	32.0	0.75	11.0	0.33	0.12	0.03	1.14	0.11	0.13	0.32
TA-4 (Footslope: Typic Paleudult)											
Ae	0–14	28.1	0.57	9.54	0.31	0.26	0.03	0.76	0.11	0.05	0.04
Bt1	14–60	28.0	1.14	9.61	0.31	0.11	0.04	0.67	0.09	0.04	0.04
Bt2	60–92	24.6	1.72	9.87	0.31	0.21	0.03	0.43	0.11	0.04	0.09
Bt3	92–125	29.3	1.68	8.36	0.37	0.20	0.03	0.46	0.12	0.05	0.08
Bt4	125–160	31.4	1.90	10.1	0.34	0.20	0.03	0.57	0.13	0.05	0.08
BC1	160–200	29.0	1.15	10.2	0.38	0.20	0.04	0.79	0.14	0.05	0.15
BC2	200–240	30.2	1.07	11.6	0.35	0.14	0.04	1.12	0.11	0.06	0.26
BC3	240–280	28.8	1.59	11.5	0.34	0.21	0.03	1.03	0.12	0.04	0.25
C	280–300	31.0	1.57	10.6	0.37	0.20	0.03	1.28	0.13	0.06	0.24
Mudstone saprolite (toeslope)		49.5	20.6	5.42	8.01	0.77	0.75	0.22	0.38	0.08	0.06

Pedons TA-3 and TA-4 are considerably less than those of Pedons TA-1 and TA-2 and could be attributed to smaller amounts of serpentine minerals within Pedons TA-3 and TA-4. Nevertheless, total Ni, which occurs primarily in the structures of serpentine minerals, shows a general increase with depth in the four pedons (Table 2). This is probably due to the greater intensity and duration of weathering and consequent release and removal of Ni from horizons nearer to the soil surface. The total Cr contents are ~10 to 25 times greater in the soils of Pedons TA-1 and TA-2 than in those of Pedons TA-3 and TA-4. Levels of total Cr, which occurs most commonly in serpentinites as the accessory mineral chromite (Becquer *et al*., 2006), are more variable with depth. Nevertheless, the differences in Cr levels between soils can be attributed to mineralogical differences in parent materials. Serpentine is most abundant in Pedon TA-1, so it has the highest Cr level of all the soils. The soils in Pedons TA-3 and TA-4 contained less Cr due to the advanced stage of pedogenesis. Additionally, relatively large Si and small heavy metal contents are found in the mudstone saprolite on the toeslope.

Clay mineral compositions

The clay mineral composition also reflects the weathering trend of soils along the toposequence. The XRD patterns of clay fractions in the Bss1 horizon of the pedon TA-2 explain the clay mineralogy (Figure 5). The main reflection at 25ºC in the K-saturated clays was present at 0.71 nm (Figure 5a), and so it could contain chlorite, as the peak was reduced when heated to 550ºC (Figure 5b). On the other hand, chlorite was clearly

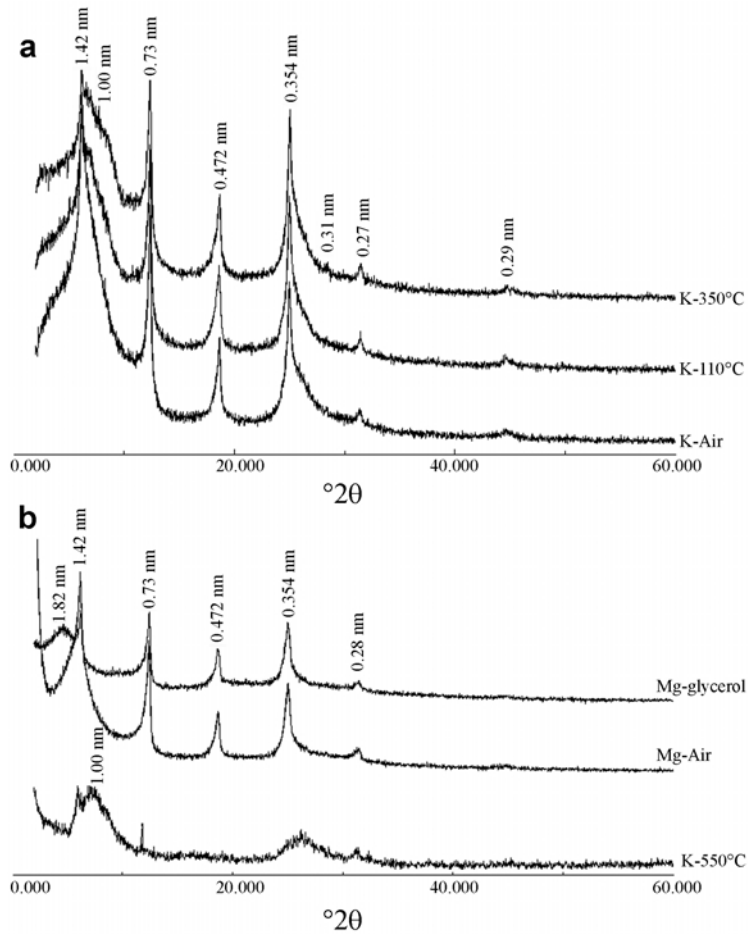

Figure 5. XRD patterns of clay fraction in the Bss1 horizon of Pedon TA-2: (a) with K- saturation treatments at 25, 110 and 350ºC; (b) with K-saturation treatment at 550ºC and with Mg-saturation treatments. CuKα radiation.

characterized by the peaks at 1.42, 0.71, 0.47 and 0.35 nm. Chlorite was present in all horizons of the four pedons, increasing with soil depth. Vermiculite was characterized both by the peak at 1.0 nm when the K-saturated clays were heated at 110ºC (Figure 5a) and by the peak at 1.42 nm when the Mg-saturated clays were solvated with glycerol (Figure 5b). The basal XRD peaks at 1.42 nm with the Mg-saturated clays intermediate between 1.2 and 1.3 nm with the K-saturated clays heated at 550ºC are characteristic of randomly interstratified chlorite-vermiculite (Sawhney, 1989; Lee *et al*., 2003), which is a chlorite-like mineral but the interlayer OH sheet of the chlorite structure is incomplete. The principle difference between randomly interstratified chlorite-vermiculite and chlorite-smectite is that the 001/001 combination peak for Mg-saturated chlorite-smectite shifts to higher spacings on glycerol treatment, while that from chlorite-vermiculite remains at 1.4 nm (Sawhney, 1989). Weaver (1956) described a number of chlorite and vermiculite mixed layers which he deduced from the relative intensities of the 1.4 nm and 0.7 nm peaks from the untreated material, as their intensities were intermediate between those expected from chlorite and vermiculite. Weaver found that on heating the sample to 400ºC, ~50% of the layers collapsed to 1.0 nm, resulting in combination peaks at 1.26 nm 001/001, 0.8 nm 001/002, 0.49 nm 002/003 and 0.349 nm 003/004, respectively. After the sample was heated at 550ºC (the temperature at which OH is removed from the chlorite and the 001 peak decreases to 1.38 nm), the 001/001 combination peak decreased from 1.26 nm to 1.16 nm. Similarly, Heystek (1956) observed that the XRD pattern of the glycol-treated clay gave a 1.43 nm diffraction peak and its submultiples. When the sample was heated to 500ºC, however, the 001/001 combination peak decreased to ~2.0 nm, suggesting a 50:50 interstratified chlorite-vermiculite. Therefore, the mixed-layer clay minerals in this study are chlorite-vermiculite forms, not chlorite-smectite forms. No depth trend of the interstratified chlorite-vermiculite was found in any pedon, but it was always less abundant in the BC or C horizons than in their overlying horizons.

Serpentine was also identified in the clay fraction of the four soil pedons by the characteristic XRD peaks at 0.73 nm which persist with K saturation and heating to

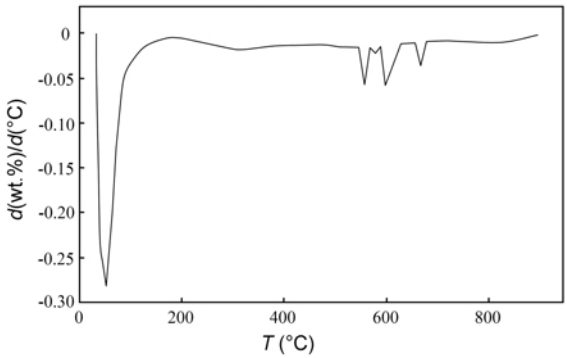

Figure 6. The thermogravimetric curve of the clay fraction of the C2 horizon of Pedon TA-1.

550ºC (Istok and Harward, 1982). Thermogravimetric data revealed the characteristic dehydroxylation temperatures of serpentine minerals and chlorite between 550 and 700ºC (Figure 6). Much more serpentine was found in the soils of Pedons TA-1 and TA-2 than those of Pedons TA-3 and TA-4, and the serpentine always increased with soil depth in each pedon. This result is in agreement with the report of Graham *et al*. (1990) which also indicated that the serpentine content decreased upwards in the profile of a serpentinitic soil in California, USA.

Smectite was identified by its 1.4 to 1.5 nm spacing after Mg saturation which expands to ~1.8 nm after glycerol solvation and which does not completely collapse to 1.0 nm after K saturation and heating to 550ºC for 2 h, suggesting the partial hydroxy-interlayering of smectite (Figure 5). This behavior was observed in other studies of serpentinite-derived soils (Wildman *et al*., 1968; Istok and Harward, 1982; Graham *et al*., 1990). The d_{060} values were used to distinguish dioctahedral (0.1510 nm) and trioctahedral (0.1538 nm) minerals (Lee *et al*., 2003). The XRD pattern for the clay fraction in the Bss1 horizon of Pedon TA-2 has a moderate peak of 0.1536 nm and a relatively small peak of 0.1511 nm suggesting that the trioctahedral minerals are the dominant smectites (not shown here). However, kaolinite in the mudstone saprolite of the toeslope was strongly characterized by the peaks at 0.72 and 0.354 nm with the K-saturated clays at 25, 110 and 350ºC, but the 0.354 nm reflection is strongly reduced when the K-saturated clays were heated at 550ºC (Figure 7). Additionally, illite was much more abundant in the mudstone saprolite on the toeslope than that on any other landscape positions along the toposequence. In general, chlorite, chlorite-vermiculite interstratified minerals, vermiculite, smectite and serpentine are the dominant clay minerals in the four soil pedons, and the appreciable amounts of kaolinite and quartz showed consistent trends through the soil profiles (Table 3). The soils of Pedons TA-1 and TA-2 contained much more smectite and serpentine, which were always predominant in the young soils derived from serpentinic rocks (Rabenhorst *et al*., 1982); however, vermiculite increased gradually in Pedons TA-3 and TA-4.

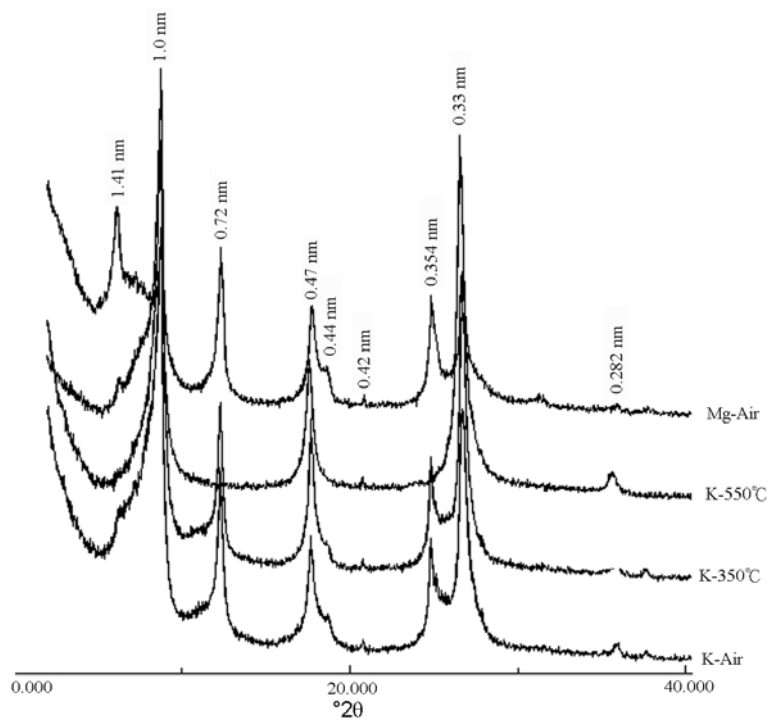

Figure 7. XRD patterns of clay fraction of the mudstone saprolite in the toeslope. CuKα radiation.

Table 3. Composition and semi-quantitative analysis of clay mineral composition in the four soil pedons[1].

Horizon	Depth (cm)	CHL	SME	C-V	VER	SER	KAO	QZ	Ill
TA-1 (Summit: Typic Udorthent)									
Aa	0–18	++[2]	+++	+	+	+	-	+	-
C1	18–51	+++	++	+	+	++	–	–	–
C2	51–90	+++	++	+	+	+	–	–	–
TA-2 (Shoulder: Typic Hapludert)									
Aa	0–10	++	+++	+	+	+	+	+	–
AB	10–30	++	+	+	+	+	–	+	–
Bss1	30–65	++	++	++	++	+	+	+	–
Bss2	65–94	++	++	++	+	++	–	+	–
Bss3	94–120	++	++	++	+	++	–	+	–
Bss4	120–145	+++	++	++	+	++	–	+	–
Bss5	145–165	+++	++	+	+	++	–	+	–
BC1	165–200	+++	+	+	+	++	–	+	–
BC2	>200	+++	+	+	+	++	–	+	–
TA-3 (Backslope: Typic Paleudalf)									
Ae	0–19	+	–	+	++	–	+	+	–
Bt1	19–48	+	–	++	++	–	+	+	–
Bt2	48–72	+	–	++	++	–	+	+	–
Bt3	72–101	+	–	+	++	–	+	+	–
Bt4	101–140	+	–	+	+	–	+	+	–
Bt5	140–170	++	–	++	+	–	+	+	–
Bt6	170–200	++	–	+	+	–	–	+	–
BC1	200–240	++	–	+	+	+	–	–	–
BC2	240–280	+++	–	+	+	+	–	–	–
C	280–300	+++	–	–	+	+	–	–	–
TA-4 (Footslope: Typic Paleudult)									
Ae	0–14	+	–	+	++	–	+	+	–
Bt1	14–60	+	–	+	++	–	+	+	–
Bt2	60–92	+	–	+	++	–	+	+	–
Bt3	92–125	+	–	++	++	–	+	+	–
Bt4	125–160	++	–	++	++	–	+	+	–
BC1	160–200	++	–	++	+	+	+	+	–
BC2	200–240	++	–	+	+	+	–	+	–
BC3	240–280	++	–	+	+	+	–	+	–
C	280–300	++	–	+	+	+	–	+	+
Mudstone saprolite (toeslope)									
		+++	–	–	+	–	+++	+	++

[1] CHL: chlorite; SME: smectite; C-V: chlorite and vermiculite mixture; VER: vermiculite; SER: serpentine; KAO: kaolinite; QZ: quartz; Ill: illite.
[2] +++: 25–50%; ++: 10–25%; +: <10%; –: undetectable

Mineral transformation during pedogenesis

Iron from the primary olivine and pyroxene is usually consumed by the formation of fine-grained magnetite, during metamorphism, disseminated through the serpentine (Figure 2d). The magnetite was gradually replaced by neoformed (pedogenic) Fe oxides such as goethite and hematite, which allowed free Fe accumulation during the genetic processes of the soils (Table 1). Serpentine and chlorite, identified by XRD and TG data, are the dominant primary minerals in the present soils. Under the different weathering conditions of tropical soil ecosystems such as the different landscapes along the toposequence in this study, serpentinite has initially weathered to smectite and interstratified chlorite-vermiculite by the formation of interlayer hydroxy sheets, and eventually to form thick argillic (Bt) horizons with high pedogenic Fe oxides and appreciable amounts of kaolinite and quartz (Table 3) because of the further chemical weathering of the above multilayered clay minerals. This result is in agreement with the reports (Massoura *et al.*, 2006) of mineralogical variations between 14 soils derived from serpentinitic rocks along a pedo-climatic environment gradient.

We further hypothesized the major mineralogical transformations that appear to occur during the genesis of these soils along the toposequence over serpentinitic rocks (Figure 8). Chlorite and serpentine dominated the mineral phases in the initially developed soil on the

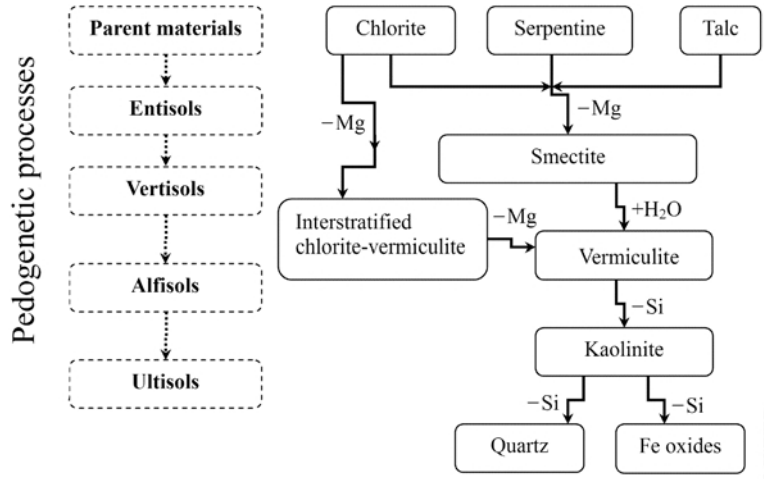

Figure 8. Clay mineral transformation of serpentinites during pedogenetic processes.

summit (Entisols); however, the mafic chlorite is highly unstable (Borchardt, 1989), and it would be expected to lose its interlayer hydroxide sheet under strong leaching and oxidizing conditions, thus forming smectite and interstratified chlorite-vermiculite which is, in turn, relatively unstable due to its trioctahedral nature in the intermediate developed soil on the shoulder (Vertisols) (Aspandiar and Eggleton, 2002a, 2002b). Bulmer and Lavkulich (1994) also indicated that smectite from serpentine was formed and altered as easily as other minerals during the earlier stage of soil development, including Entisol, Inceptisol and Vertisol. On the other hand, vermiculite was formed as a weathering product of chlorite through an intermediate interstratified chlorite-vermiculite mineral in the moderately well developed soil on the backslope (Alfisols), whereas the removal of all or portions of the interlayer hydroxide sheet within chlorite is a general weathering process that depends on the quantity of interlayer Fe^{2+}, the oxidation of Fe^{2+} to Fe^{3+}, and the subsequent removal of Fe and Mg from the interlayer hydroxide sheets. The various multilayered silicates are gradually transformed as kaolinite and quartz, which are associated with the greatest concentration of Fe_d on the footslope (Ultisols) along the toposequence. Furthermore, Mg, Ni and Cr were leached out of the soils during the pedogenetic processes.

However, the abundance of kaolinite decreased with soil depth of pedons so that mudstone at depth is unlikely to be a source of kaolinite. The mudstone saprolite on the toeslope is quite different from the soils of Pedons TA-3 and TA-4 in chemical and mineralogical compositions such as metal concentrations and serpentine minerals, indicating that the mudstone saprolites were not significantly contaminated by the above-mentioned colluvial action. From the eolian point of view, it is possible that aeolian quartz was accumulated in the soil surfaces. However, the study area is located at Hua-tung valley along Peinan River between the Central Ridge and Coastal Range of Taiwan with average elevation >1000 m in humid tropical conditions (Figure 1). These high mountains act as effective barriers to the accumulation of atmospheric dusts from the Asian continent such as mainland China, in spite of the suggestion by Simonson (1995) who reported aeolian materials having moved east from northern China to be deposited in southern Japan. Additionally, the prevailing monsoon winds of Taiwan are from southwest in summer and northeast in winter, and these wind directions are different from those reported by Simonson (1995). Therefore, aeolian action by long-distance transport is unlikely to be a significant source of quartz in the soils studied in this work. Nevertheless, lithological discontinuity was recognized through the depth functions of clay-free particle-size fractions and abrupt decreases in silt content at subsurface horizons found in all pedons (Table 1), indicating the presence of small amounts of local aeolian materials over serpentinites. This illustration is supported by Langley-Turnbaugh and Bockheim (1997) and Gunal and Ransom (2006) who identified this aeolian addition during pedogenesis.

CONCLUSIONS

Entisol on the summit, Vertisol on the shoulder, Alfisol on the backslope and Ultisol on the footslope were represented along the short-distance serpentinitic toposequence. Serpentine and chlorite are the dominant minerals in the unweathered rock. Three polymorphs of serpentine were clearly identified by microscopic textures. Magnetite, the associated mineral disseminated through the serpentine, was gradually replaced by pedogenic Fe oxides which were identified by the accumulation of Fe_d, particularly in the soils on the backslope and footslope. The total Cr and Ni contents in the soils on the summit and shoulder positions are large, while those on the backslope and footslope positions are

relatively small, because of the differences in quantity of serpentine in parent rocks and soils in the study area. Serpentine in the Entisol has initially weathered to smectite and interstratified chlorite-vermiculite, which became the dominant minerals in the Vertisol. However, vermiculite was further formed as a weathering product in the Alfisol. These various multilayered silicates are eventually transformed as kaolinite and quartz in the Ultisol. In addition, locally, aeolian materials make a small contribution in terms of quartz addition to the soils, particularly in the subsurface horizons.

ACKNOWLEDGMENTS

The authors thank the National Science Council of the Republic of China, Taiwan, for providing financial support for this research under Contract No. NSC 95-2622-E-020-009-CC3. Miss Y.H. Chang is acknowledged for her assistance in field sampling and laboratory analysis.

REFERENCES

Alexander, E.B. (1988) Morphology, fertility and classification of productive soils on serpentinised peridotite in California, U.S.A. *Geoderma*, **41**, 337–351.

Alexander, E.B., Adamson, C., Graham, R.C. and Zinke, P.J. (1989) Soils and conifer forest productivity on serpentinized peridotite of the trinity ophiolite, California. *Soil Science*, **148**, 412–423.

Aspandiar, M.F. and Eggleton, R.A. (2002a) Weathering of chlorite: I. Reactions and products in microsystems controlled by the primary mineral. *Clays and Clay Minerals*, **50**, 685–698.

Aspandiar, M.F. and Eggleton, R.A. (2002b) Weathering of chlorite: II. Reactions and products in microsystems controlled by solution avenues. *Clays and Clay Minerals*, **50**, 699–709.

Becquer, T., Rotte-Capet, S., Ghanbaja, J., Mustin, C. and Herbillon, A.J. (2006) Sources of trace metals in Ferralsols in New Caledonia. *European Journal of Soil Science*, **57**, 200–213.

Bonifacio, E., Zanini, E., Boero, V. and Franchini-Angela, M. (1997) Pedogenesis in a soil catena on serpentinite in northwestern Italy. *Geoderma*, **75**, 33–51.

Borchardt, G. (1989) Smectites. Pp. 675–727 in: *Minerals in Soil Environments*, 2nd edition (J.B. Dixon and S.B. Weed, editors). SSSA Book Series No. 1. Soil Science Society of America, Madison, Wisconsin.

Bullock, P., Fedoroff, N., Jongerius, A., Stoops, G. and Tursina, T. (1985) *Handbook for Thin Section Description*. Waine Research Publishers, Albrighton, England. 152 pp.

Bulmer, C.E. and Lavkulich, L.M. (1994) Pedogenic and geochemical processes of ultramafic soils along a climatic gradient in southwestern British Columbia. *Canadian Journal of Soil Science*, **74**, 165–177.

Burt, R., Fillmore, M., Wilson, M.A., Gross, E.R., Langridge, R.W. and Lammers, D.A. (2001) Soil properties of selected pedons on ultramafic rocks in Klamath Mountains, Oregon. *Communications in Soil Science and Plant Analysis*, **32**, 2145–2175.

Caillaud, J., Proust, D., Righi, D. and Martin, F. (2004) Fe-rich clays in a weathering profile developed from serpentinite. *Clays and Clay Minerals*, **52**, 779–791.

Caillaud, J., Proust, D. and Righi, D. (2006) Weathering sequences of rock-forming minerals in a serpentinite: influence of microsystems on clay mineralogy. *Clays and Clay Minerals*, **54**, 87–100.

Cheshire, M. and Güven, N. (2005) Conversion of chrysotile to a magnesian smectite. *Clays and Clay Minerals*, **53**, 155–161.

Dirven, J.M.C., van Schuylenborch, J. and van Breemen, N. (1976) Weathering of serpentinite in Matanzas Province, Cuba: Mass transfer calculations and irreversible reaction pathways. *Soil Science Society of America Journal*, **40**, 901–907.

Dixon, J.B. (1989) Kaolin and serpentine group minerals. Pp. 467–526 in: *Minerals in Soil Environments*, 2nd edition (J.B. Dixon and S.B. Weed, editors). SSSA Book Series No. **1**. Soil Science Society of America, Madision, Wisconsin.

Garnier, J., Quantin, C., Martins, E.s. and Becquer, T. (2006) Solid speciation and availability of chromium in ultramafic soils from Niquelândia, Brazil. *Journal of Geochemical Exploration*, **88**, 206–209.

Gee, G.W. and Bauder, J.W. (1986) Particle-size analysis. Pp. 383–411 in: *Methods of Soil Analysis*, Part 1. 2nd edition (A.L. Page, R.H. Miller and D.R. Keeney, editors). Agronomy Monograph **9**. American Society of Agronomy and Soil Science Society of America, Madison, Wisconsin.

Golighty, J.P. (1981) Nickeliferous laterite deposits. *Economic Geology*, **75**, 710–735.

Graham, R.C., Diallo, M.M. and Lund, L.J. (1990) Soils and mineral weathering on phyllite colluviun and serpentinite in northwestern California. *Soil Science Society of America Journal*, **54**, 1682–1690.

Gunal, H. and Ransom, M.D. (2006) Genesis and micromorphology of loess-derived soils from central Kansas. *Catena*, **65**, 222–236.

Hamblin, W.K. (1992) *Earth's Dynamic Systems*, 6th edition. Macmillan Publishers, New York, 647 pp.

Heystek, H. (1956) Vermiculite as a member in mixed-layer minerals. *Clays and Clay Minerals*, **4**, 429–434.

Ho, C.S. (1988) *An Introduction to the Gof Taiwan: Explanatory Text of the Geologic Map of Taiwan,* 2nd edition. Centenary Geological Survey, Taipei, Taiwan, 192 pp.

Hseu, Z.Y. (2006) Concentration and distribution of chromium and nickel fractions along a serpentinitic toposequence. *Soil Science*, **171**, 341–353.

Istok, J.D. and Harward, M.E. (1982) Influence of soil moisture on smectite formation in soils derived from serpentinite. *Soil Science Society of America Journal*, **46**, 1106–1108.

Johns, W.D., Grim, R.E. and Bradley, W.F. (1954) Quantitative estimations of clay minerals by diffraction methods. *Journal of Sedimentary Petrology*, **24**, 242–251.

Kahle, M., Kleber, M. and Jahn, R. (2002) Review of XRD-based quantitative analyses of clay minerals in soils: the suitability of mineral intensity factors. *Geoderma*, **109**, 191–205.

Langley-Turnbaugh, S.J. and Bockheim, J.G. (1997) Time-dependent changes in pedogenic processes on marine terraces in coastal Oregon. *Soil Science Society of America Journal*, **61**, 1428–1440.

Lee, B.D., Sears, S.K., Graham, R.C., Amrhein, C. and Vali, H. (2003) Secondary mineral genesis from chlorite and serpentine in an ultramafic soil toposequence. *Soil Science Society of America Journal*, **67**, 1309–1317.

Lee, B.D., Graham, R.C., Laurent, T.E. and Amrhein, C. (2004) Pedogenesis in a wetland meadow and surrounding serpentinitic landslide terrain, northern California, USA. *Geoderma*, **118**, 303–320.

Massoura, S.T., Echevarria, G., Becquer, T., Ghanbaja, J., Leclerc-Cessac, E. and Morel, J. (2006) Control of nickel availability by nickel bearing minerals in natural and anthropogenic soils. *Geoderma*, **136**, 28–37.

McLean, E.O. (1982) Soil pH and lime requirement. Pp.

199–224 in: *Methods of Soil Analysis, Part 2, Chemical and Microbiological Properties*, 2nd edition (A.L. Page, R.H. Miller and D.R. Keeney, editors). Agronomy Monograph **9**. American Society of Agronomy and Soil Science Society of America, Madison, Wisconsin.

Mehra, O.P. and Jackson, M.J. (1960) Iron oxides removed from soils and clays by a dithionite-citrate system buffered with sodium bicarbonate. *Clays and Clay Minerals*, **7**, 317–327.

Nelson, D.W. and Sommers, L.E. (1982) Total carbon, OC and organic matter. Pp. 539–557 in: *Methods of Soil Analysis, Part 2, Chemical and Microbiological Properties*, 2nd edition (A.L. Page, R.H. Miller and D.R. Keeney, editors). Agronomy Monograph **9**. American Society of Agronomy and Soil Science Society of America, Madison, Wisconsin.

Nesse, W.D. (2000) Sheet silicates. Pp. 235–260 in: *Introduction to Mineralogy*. Oxford University Press, New York.

Rabenhorst, M.C., Foss, J.E. and Fanning, D.S. (1982) Genesis of Maryland soils formed from serpentinite. *Soil Science Society of America Journal*, **46**, 607–616.

Rhoades, J.D. (1982) Cation exchange capacity. Pp. 149–157 in: *Methods of Soil Analysis, Part 2, Chemical and Microbiological Properties*, 2nd edition (A.L. Page, R.H. Miller and D.R. Keeney, editors). Agronomy Monograph **9**. American Society of Agronomy and Soil Science Society of America, Madison, Wisconsin.

Sawhney, B.L. (1989) Interstratification in layer silicates. Pp. 789–828 in: *Minerals in Soil Environments*, 2nd edition (J.B. Dixon and S.B. Weed, editors). SSSA Book Series No. **1**. Soil Science Society of America, Madision, Wisconsin.

Schreier, H., Omueti, J.A. and Lavkulich, L.M. (1987) Weathering processes of asbestos-rich serpentinitic sediments. *Soil Science Society of America Journal*, **51**, 993–999.

Simonson, R.W. (1995) Airborne dust and its significance to soils. *Geoderma*, **65**, 1–43.

Soil Survey Staff (2006) *Keys to Soil Taxonomy*, 10th edition. Natural Resources Conversation Services, United States Department of Agriculture, Washington, D.C., 332 pp.

Weaver, C.E. (1956) The distribution and identification of mixed-layer clays in sedimentary rocks. *American Mineralogists*, **41**, 202–221.

Whittaker, R.H. (1954) The ecology of serpentine soils. IV. The vegetation response to serpentine soils. *Ecology*, **35**, 275–288.

Wildman, W.E., Jackson, M.L. and Whittig, L.D. (1968) Iron-rich montmorillonite formation in soils derived from serpentinite. *Soil Science Society of America Proceedings*, **32**, 787–794.

Wilson, M.J. and Berrow, M.L. (1978) The mineralogy and heavy metal content of some serpentinite soils in northeast Scotland. *Chemie der Erde*, **37**, 181–205.

(*Received 15 April 2006; revised 6 December 2006; Ms. 1164*)